EDUSCHOOL JOURNAL OF COMPUTER SCIENCE RESEARCH STUDIES (EJCSRS)

(Open Access, Double-Blind Peer Reviewed Journal)

ISSN Online: ISSN Print

Quantum Error Correction: Surface And Topological Codes

Raji N

Assistant Professor, Department of Computer Science, Yuvakshatra Institute of Management Studies (YIMS), Mundur, India.

Article information

Received: 10th December 2025
Received in revised form: 11th January 2026
Accepted: 13th February 2026
Available online: 12th March 2026

Volume: 1
Issue: 1
DOI: https://doi.org/10.5281/zenodo.18975936

Abstract

Quantum error correction (QEC) represents a critical enabler for fault-tolerant quantum computing, protecting fragile quantum states from decoherence and operational errors. This paper provides a comprehensive analysis of leading quantum error correction schemes, focusing on surface codes and topological codes within the context of Noisy Intermediate-Scale Quantum (NISQ) era processors. We examine the theoretical foundations of stabilizer codes, compare surface code implementations with code distances ranging from d=3 to d=17, and analyze topological codes including toric codes and color codes. Our investigation encompasses syndrome extraction circuits, logical qubit encoding strategies, and threshold analysis for contemporary quantum hardware platforms. Performance metrics reveal that surface codes achieve error thresholds of approximately 1% with realistic noise models, while topological codes offer architectural advantages for specific qubit connectivity constraints. We discuss implementation challenges on current NISQ processors including IBM Quantum, Google Sycamore, and IonQ systems, addressing qubit overhead, gate fidelity requirements, and decoding algorithms. This analysis provides insights for selecting appropriate error correction schemes based on application requirements and hardware capabilities.

Keywords:- Quantum Error Correction, Surface Codes, Topological Codes, NISQ Processors, Stabilizer Codes, Fault Tolerance

I. INTRODUCTION

Quantum computers promise exponential speedups for specific computational problems including integer factorization, quantum simulation, and optimization [1]. However, quantum systems inherently suffer from decoherence and operational errors that corrupt quantum information before algorithms can complete. Unlike classical bits that experience only bit-flip errors, qubits undergo continuous errors in infinite-dimensional Hilbert space, requiring fundamentally different error correction strategies [2].

Quantum error correction (QEC) addresses these challenges by encoding logical qubits into entangled states of multiple physical qubits, enabling error detection and correction without measuring quantum information directly. The threshold theorem establishes that arbitrary-length quantum computation becomes possible when physical error rates fall below a specific threshold, typically 10^{-3} to 10^{-2} depending on the code and error model [3]. This threshold represents the critical transition between exponentially growing errors and arbitrarily accurate quantum computation through increased code distance.

Surface codes have emerged as the leading QEC candidates due to their high error thresholds, nearest-neighbor qubit connectivity requirements, and efficient decoding algorithms [4]. Topological codes, including toric codes and color codes, offer theoretical advantages in certain architectural scenarios and provide alternative approaches for specific qubit connectivity graphs [5]. This paper examines these codes within the context of NISQ-era processors, where limited qubit counts and coherence times constrain practical error correction implementations.

The remainder of this paper is organized as follows: Section II reviews stabilizer formalism and QEC fundamentals. Section III analyzes surface code architectures and performance. Section IV examines topological code variants. Section V discusses NISQ implementation challenges. Section VI presents comparative analysis and deployment strategies. Section VII concludes with future research directions.

II. STABILIZER CODES AND QEC FUNDAMENTALS

A. Stabilizer Formalism

Stabilizer codes form the foundation for most practical QEC schemes, utilizing the stabilizer formalism to detect errors through syndrome measurements [6]. An [[n,k,d]] stabilizer code encodes k logical qubits into n physical qubits with code distance d, where the code can detect up to d-1 errors and correct $\lfloor(d-1)/2\rfloor$ errors. The stabilizer group S consists of commuting Pauli operators that leave the code space invariant:

$$S = < g^1, g^2, \ldots, g_{n}{}^{-}{}_{k} > \text{ where } g_i \in \{I, X, Y, Z\} \otimes {}^{n} \quad (1)$$

Syndrome measurements determine the eigenvalues of stabilizer generators without collapsing the quantum state, revealing which error occurred. The logical operators $\bar{X}$ and $\bar{Z}$ commute with all stabilizers but anti-commute with each other, forming the basis for encoded quantum information [7].

B. Error Models and Noise Channels

Quantum errors manifest through decoherence processes describable by quantum channels. The depolarizing channel models symmetric errors where X, Y, and Z errors occur with equal probability p/3 each:

$$\rho \rightarrow (1\text{-}p)\rho + (p/3)(X\rho X + Y\rho Y + Z\rho Z) \quad (2)$$

More realistic models include amplitude damping representing energy relaxation (T_1 decay) and phase damping modeling dephasing (T_2 decay). Contemporary superconducting qubits exhibit T_1 times of 50-200μs and T_2 times of 30-150μs, imposing stringent constraints on error correction cycles [8]. Two-qubit gate fidelities typically range from 99.0% to 99.9%, with measurement fidelities exceeding 99.5%.

C. Syndrome Extraction and Decoding

Extracting error syndromes requires ancilla qubits and controlled operations that entangle ancillas with data qubits [9]. Each stabilizer generator measurement uses one ancilla qubit initialized in $|0\rangle$, followed by controlled-NOT gates implementing the Pauli operator pattern, then measuring the ancilla in the computational basis. Decoding algorithms interpret syndrome patterns to determine the most likely error chain. Minimum-weight perfect matching (MWPM) provides efficient near-optimal decoding for surface codes with $O(n^3)$ complexity, while machine learning decoders achieve improved performance through neural networks trained on syndrome distributions [10].

III. SURFACE CODE ARCHITECTURES

A. Planar Surface Code Structure

The planar surface code arranges physical qubits on a two-dimensional lattice with data qubits at vertices and ancilla qubits at faces and edges [4]. For code distance d, the surface code requires $n = 2d^2 - 2d + 1$ physical qubits to encode one logical qubit. The stabilizer generators consist of four-qubit X-type plaquette operators and four-qubit Z-type star operators:

$$A_p = X_1X_2X_3X_4 \text{ (plaquette stabilizers)} \quad (3)$$

$$B_s = Z_1Z_2Z_3Z_4 \text{ (star stabilizers)} \quad (4)$$

Boundary conditions modify stabilizer weights at edges to two or three qubits. The logical $\bar{X}$ operator consists of X operators along a horizontal path from left to right boundary, while logical $\bar{Z}$ comprises Z operators along a vertical path from top to bottom [11]. This construction requires only nearest-neighbor connectivity, making it compatible with superconducting qubit architectures.

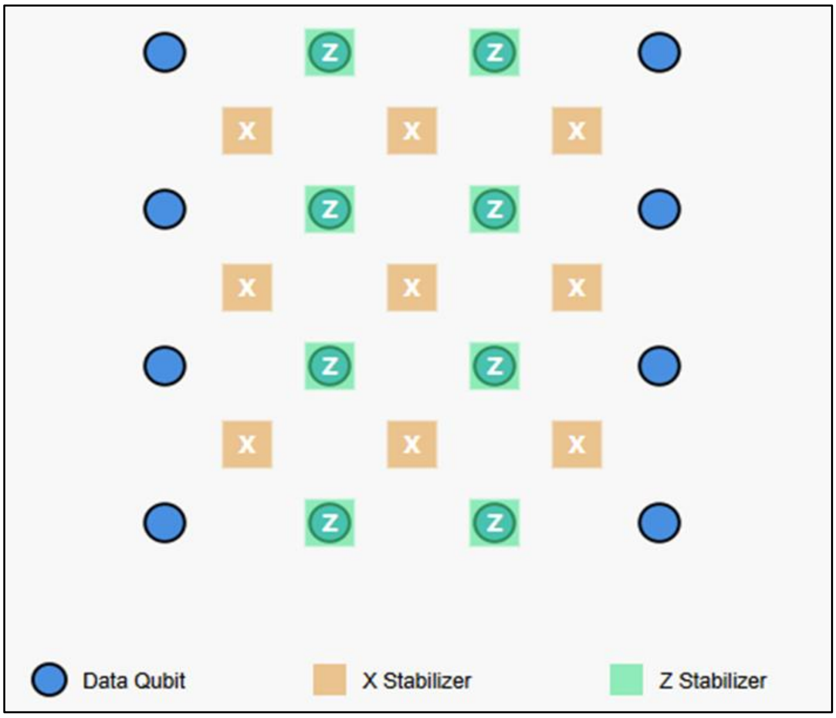

Fig. 1: Surface code lattice structure(distance d=3) showing data qubits (blue circles), X-type stabilizers (orange), and Z-type stabilizers (green) for a distance d=3 code

B. Error Thresholds and Performance

Surface codes achieve remarkable error thresholds approaching 1% for idealized circuit-level noise [12]. Table I presents threshold values under different noise models and decoding strategies. The code distance d determines the number of errors that can be corrected; d=3 provides basic error correction, while d=17 enables correction of up to 8 errors per syndrome extraction cycle.

Table 1. Surface Code Error Thresholds]

Noise Model	Decoder	Threshold (%)
Depolarizing	MWPM	1.09
Circuit-level	MWPM	0.57
Biased noise (Z)	MWPM	2.93
Circuit-level	ML decoder	0.68

The logical error rate PL decreases exponentially with code distance above threshold: PL ≈ A(p/pth)^((d+1)/2), where p represents the physical error rate and pth denotes the threshold. For d=5 at p=0.1%, the logical error rate reaches approximately 10^{-6}, sufficient for small quantum algorithms [13].

C. Logical Gate Implementation

Implementing logical gates on surface codes requires fault-tolerant protocols. Logical Pauli gates execute through transversal operations on physical qubits. The logical Hadamard gate transposes the lattice, exchanging X and Z stabilizers. The logical CNOT gate combines two surface code patches through lattice surgery, creating temporary boundaries and merging stabilizer measurements [14]. Non-Clifford gates like the T gate require magic state distillation, consuming additional qubits and increasing circuit depth by 10-100×. Recent innovations in lattice surgery enable more efficient multi-qubit operations while maintaining fault tolerance [15].

IV. TOPOLOGICAL CODES

A. Toric Code Structure

The toric code represents the prototypical topological quantum code, defined on a torus topology with periodic boundary conditions [16]. For an L×L lattice, the toric code encodes k=2 logical qubits into $n=2L^2$ physical qubits with code distance d=L. The stabilizer generators mirror the surface code structure but include periodic boundaries that eliminate edge effects.

Logical operators in the toric code correspond to non-contractible loops around the torus. Two independent $\bar{X}$ operators wrap horizontally and vertically, with corresponding $\bar{Z}$ operators completing the logical qubit basis. The code distance equals the minimum loop length, providing inherent protection against local errors. However, implementing true toroidal topology on planar quantum hardware requires long-range connectivity or virtual implementations through teleportation [17].

B. Color Codes

Color codes define stabilizers on lattices with three-colorable faces, supporting transversal implementation of non-Clifford gates [18]. The triangular color code uses a hexagonal lattice where each plaquette is colored red, green, or blue such that adjacent plaquettes have different colors. Stabilizers consist of six-qubit operators applied to qubits surrounding each plaquette:

$$S^c = X^c{}_1 X^c{}_2 X^c{}_3 X^c{}_4 X^c{}_5 X^c{}_6 \text{ or } Z^c{}_1 Z^c{}_2 Z^c{}_3 Z^c{}_4 Z^c{}_5 Z^c{}_6 \quad (5)$$

The color code's primary advantage lies in transversal implementation of the logical T gate, eliminating magic state distillation overhead [19]. However, color codes require higher qubit connectivity compared to surface codes, with degree-6 nodes in the triangular lattice versus degree-4 for surface codes. This connectivity constraint limits near-term implementations on current hardware architectures.

C. Comparative Analysis

Surface codes offer superior error thresholds and efficient decoding for nearest-neighbor architectures, making them the practical choice for superconducting and silicon-based quantum processors. Toric codes provide theoretical elegance and simplified logical operator structure but require non-planar connectivity. Color codes enable transversal non-Clifford gates at the cost of increased qubit connectivity and slightly lower error thresholds around 0.1-0.2% [20]. Selection between codes depends on hardware topology, available connectivity, and application requirements for logical gate implementations.

V. NISQ IMPLEMENTATION CHALLENGES

A. Qubit Overhead Requirements

Practical quantum error correction demands substantial qubit overhead. A distance-5 surface code requires 49 physical qubits to encode one logical qubit, while distance-17 codes use 577 physical qubits. Current NISQ processors provide 50-1000 qubits, limiting error-corrected implementations to small code distances or single logical qubits [21]. IBM Quantum Eagle processor with 127 qubits can implement d=5 surface codes for two logical qubits, insufficient for most quantum algorithms.

B. Gate Fidelity and Coherence Requirements

Operating below the error threshold requires high-fidelity gates and long coherence times. For surface codes with 0.5% threshold, physical gate errors must remain below 0.1% to achieve logical error suppression with d=5 [22]. Contemporary superconducting qubits approach this regime with two-qubit gate fidelities of 99.4-99.9%. However, syndrome extraction circuits introduce additional errors through measurement and ancilla qubit operations, effectively reducing the threshold. Rapid syndrome extraction cycles within coherence time T_2 enable multiple error correction rounds before decoherence dominates.

C. Decoder Latency Constraints

Real-time decoding presents significant challenges for fault-tolerant quantum computing. Classical decoding algorithms must process syndrome data and determine corrections within the error correction cycle time, typically 1-10μs for superconducting qubits [23]. Minimum-weight perfect matching achieves $O(n^3)$ complexity but requires optimization for real-time performance. GPU-accelerated decoders and FPGA implementations reduce latency to microseconds for small code distances. Machine learning decoders offer improved accuracy but face inference latency challenges. Ongoing research explores in-situ decoding with low-latency classical control systems integrated with quantum processors.

VI. COMPARATIVE ANALYSIS AND DEPLOYMENT

A. Platform-Specific Implementations

IBM Quantum systems utilize heavy-hexagon connectivity optimized for surface code implementations [24]. Google's Sycamore processor demonstrated quantum error correction with the surface code, achieving below-threshold performance for d=3 and d=5 codes. IonQ trapped-ion systems offer all-to-all connectivity enabling flexible code implementations including color codes. Each platform presents distinct trade-offs between qubit count, connectivity, and gate fidelities influencing optimal code selection.

B. Application-Driven Code Selection

Quantum applications exhibit varying error correction requirements. Quantum chemistry simulations benefit from surface codes due to high Clifford gate content and MWPM decoding efficiency. Cryptographic applications requiring T-depth optimization may favor color codes for transversal T gates. Quantum error detection codes provide intermediate solutions for NISQ algorithms, detecting errors without full correction to mitigate decoherence [25]. Hybrid approaches combining classical error mitigation with lightweight QEC enable near-term applications on existing hardware.

VII. CONCLUSION

Quantum error correction represents an essential technology for scaling quantum computers beyond NISQ limitations toward fault-tolerant quantum computation. Surface codes offer the most practical near-term path with high error thresholds, nearest-neighbor connectivity, and efficient decoding. Topological codes including toric and color codes provide architectural alternatives with specific advantages for logical gate implementations. Current NISQ processors approach the regime where small-scale error correction becomes feasible, with gate fidelities and coherence times sufficient for d=3 to d=5 codes.

Future developments will focus on increasing physical qubit counts to support larger code distances, improving gate fidelities to operate further below threshold, and developing faster decoding algorithms for real-time error correction. Architectural innovations including fusion-based quantum computing and measurement-based models may enable more efficient error correction implementations. The convergence of improved hardware, optimized codes, and advanced decoding will enable fault-tolerant quantum algorithms capable of solving problems intractable for classical computers.

Standardized benchmarks and metrics for comparing QEC performance across platforms will accelerate progress toward practical quantum computers. As quantum systems transition from NISQ devices to fully fault-tolerant machines, quantum error correction will transform from a research topic to an engineering discipline enabling reliable quantum computation at scale.

REFERENCES

[1] M. A. Nielsen and I. L. Chuang, Quantum Computation and Quantum Information. Cambridge University Press, 2010.

[2] P. W. Shor, "Scheme for reducing decoherence in quantum computer memory," Physical Review A, vol. 52, no. 4, pp. R2493-R2496, Oct. 1995.

[3] E. Knill, R. Laflamme, and W. H. Zurek, "Resilient quantum computation: Error models and thresholds," Proceedings of the Royal Society A, vol. 454, no. 1969, pp. 365-384, 1998.

[4] G. Fowler et al., "Surface codes: Towards practical large-scale quantum computation," Physical Review A, vol. 86, no. 3, p. 032324, Sep. 2012.

[5] H. Bombin and M. A. Martin-Delgado, "Topological quantum distillation," Physical Review Letters, vol. 97, no. 18, p. 180501, Nov. 2006.

[6] D. Gottesman, "Stabilizer codes and quantum error correction," PhD dissertation, California Institute of Technology, 1997.

[7] R. Calderbank and P. W. Shor, "Good quantum error-correcting codes exist," Physical Review A, vol. 54, no. 2, pp. 1098-1105, Aug. 1996.

[8] F. Arute et al., "Quantum supremacy using a programmable superconducting processor," Nature, vol. 574, no. 7779, pp. 505-510, Oct. 2019.

[9] D. P. DiVincenzo and P. W. Shor, "Fault-tolerant error correction with efficient quantum codes," Physical Review Letters, vol. 77, no. 15, pp. 3260-3263, Oct. 1996.

[10] P. Baireuther et al., "Machine-learning-assisted correction of correlated qubit errors," Quantum, vol. 2, p. 48, Jan. 2018.

[11] G. Fowler, "Minimum weight perfect matching of fault-tolerant topological quantum error correction in average O(1) parallel time," Quantum Information and Computation, vol. 15, no. 1-2, pp. 145-158, 2015.

[12] G. Fowler, A. C. Whiteside, and L. C. L. Hollenberg, "Towards practical classical processing for the surface code," Physical Review Letters, vol. 108, no. 18, p. 180501, May 2012.

[13] Google Quantum AI, "Exponential suppression of bit or phase errors," Nature, vol. 595, no. 7867, pp. 383-387, Jul. 2021.

[14] Horsman et al., "Surface code quantum computing by lattice surgery," New Journal of Physics, vol. 14, no. 12, p. 123011, Dec. 2012.

[15] Litinski, "A game of surface codes: Large-scale quantum computing with lattice surgery," Quantum, vol. 3, p. 128, Mar. 2019.

[16] Y. Kitaev, "Fault-tolerant quantum computation by anyons," Annals of Physics, vol. 303, no. 1, pp. 2-30, Jan. 2003.

[17] R. Raussendorf and J. Harrington, "Fault-tolerant quantum computation with high threshold in two dimensions," Physical Review Letters, vol. 98, no. 19, p. 190504, May 2007.

[18] H. Bombin and M. A. Martin-Delgado, "Topological computation without braiding," Physical Review Letters, vol. 98, no. 16, p. 160502, Apr. 2007.
[19] J. Landahl, J. T. Anderson, and P. R. Rice, "Fault-tolerant quantum computing with color codes," arXiv:1108.5738, 2011.
[20] K. Sahay et al., "High threshold codes for neutral atom qubits with biased erasure errors," Physical Review X, vol. 13, no. 4, p. 041013, Oct. 2023.
[21] J. Preskill, "Quantum computing in the NISQ era and beyond," Quantum, vol. 2, p. 79, Aug. 2018.
[22] Chamberland et al., "Building a fault-tolerant quantum computer using concatenated cat codes," PRX Quantum, vol. 3, no. 1, p. 010329, Feb. 2022.
[23] C. Ryan-Anderson et al., "Realization of real-time fault-tolerant quantum error correction," Physical Review X, vol. 11, no. 4, p. 041058, Dec. 2021.
[24] M. Takita et al., "Demonstration of weight-four parity measurements in the surface code architecture," Physical Review Letters, vol. 117, no. 21, p. 210505, Nov. 2016.
[25] K. Temme et al., "Error mitigation for short-depth quantum circuits," Physical Review Letters, vol. 119, no. 18, p. 180509, Nov. 2017.